Cannabinoid CB1 receptors and ligands in vertebrate retina: Localization and function of an endogenous signaling system

Alex Straiker*[†], Nephi Stella[‡], Daniele Piomelli[‡], Ken Mackie[§], Harvey J. Karten*, and Greg Maguire[¶]

Departments of *Neurosciences and [¶]Ophthalmology, University of California School of Medicine, San Diego, CA 92093; [‡]The Neurosciences Institute, San Diego, CA 92121; and [§]Departments of Anesthesiology, and Physiology and Biophysics, University of Washington, Seattle, WA 98195

CB1, a cannabinoid receptor enriched in neuronal tissue, was found in high concentration in retinas of rhesus monkey, mouse, rat, chick, goldfish, and tiger salamander by using a subtype-specific polyclonal antibody. Immunolabeling was detected in the two synaptic layers of the retina, the inner and outer plexiform layers, of all six species examined. In the outer plexiform layer, CB1 was located in and/or on cone pedicles and rod spherules. Labeling was detected in some amacrine cells of all species and in the ganglion cells and ganglion cell axons of all species except fish. In addition, sparse labeling was found in the inner and/or outer segments of the photoreceptors of monkey, mouse, rat, and chick. Using GC/MS to detect possible endogenous cannabinoids, we found 3 nmol of 2-arachidonylglycerol per g of tissue, but no anandamide was detectable. Cannabinoid receptor agonists induced a dramatic reduction in the amplitude of voltage-gated L-type calcium channel currents in identified retinal bipolar cells. The presence and distribution of the CB1 receptor, the large amounts of 2-arachidonylglycerol found, and the effects of cannabinoids on calcium channel activity in bipolar cells suggest a substantive role for an endogenous cannabinoid signaling system in retinal physiology, and perhaps vision in general.

Cannabinoids are the principal psychoactive component of marijuana and hashish, acting on an intrinsic G protein-coupled receptor in nervous tissue that normally responds to endogenous ligands such as anandamide (arachidonylethanolamide, or AEA) (1). Despite considerable recent progress, the mechanisms of cannabinoid action in the body remain poorly understood, particularly in the case for the role of cannabinoids in vision. Published research and case studies as well as a host of anecdotal reports describe numerous effects on visual perception including altered thresholds of light detection and glare recovery (2–4). The possible loci within the retina and/or brain responsible for these perceptual changes are unknown. Our report may identify one of the major sites responsible for the alterations in the visual world of some cannabinoid users.

The first cannabinoid receptor, CB1, was cloned in 1990 (5). Since then the CB1 receptor has been found to be expressed at high levels in specific brain regions (6). Putative endogenous ligands have been identified: anandamide (1) and 2-arachidonylglycerol (2-AG) (7). Endogenous cannabinoids have been shown to produce effects on memory, signaling pathways, and the perception of pain, (8–14) and have even been found to inhibit dopamine release in the leech (15), implying an inveterate history as a neuromodulatory system.

Recent evidence suggests that cannabinoid receptors are found in the retina, with one study demonstrating an anandamide-induced inhibition of dopamine release (16) and another study showing expression of CB1 mRNA through *in situ* labeling in embryonic rat retina (17). Recently, Porcella *et al.* (18) have found mRNA for CB1 in retina, by using reverse transcription–PCR. However neither precise localization of the expression of CB1 receptor protein, nor localization of cannabinoids, has been reported in vertebrate retina.

The goal of our study was to determine the cellular localization of cannabinoid receptors and the presence of putative endogenous ligands anandamide and 2-AG in the vertebrate retina and to explore the physiology of cannabinoid receptor activation. Here we report that CB1 receptors are found in the outer plexiform layer (OPL) and inner plexiform layer (IPL) of the six species examined: the rhesus monkey, the mouse, the rat, the chick, the goldfish, and the tiger salamander. We have determined that 2-AG, the endogenous ligand for CB1, and palmitylethanolamide (PEA), a putative endogenous ligand for the CB2 receptor (19), are present in rat retina at concentrations similar to those seen elsewhere in the brain, but that the rat retina does not contain anandamide. Further, voltage-gated calcium channel activity in retinal bipolar cells of the tiger salamander was modulated by activation of CB1 receptors. These data strongly suggest that an endogenous cannabinoid signaling system is present in the vertebrate retina, and that it may act presynaptically to regulate glutamatergic synaptic transmission.

Materials and Methods

Immunohistochemistry. Eyes from two adult mice (strain C57/Black6), five adult Sprague–Dawley rats, two chicks, three larval tiger salamanders, one goldfish, and one adult rhesus monkey were used in these experiments. Mice and rats were anesthetized (210 mg/kg and 120 mg/kg sodium pentobarbital, respectively, i.p.) and then killed. Chicks were anesthetized by a combined ketamine (80 mg/kg) and xylazine (16 mg/kg) injection and then killed. All animals were sacrificed by decapitation. The eye was promptly dissected out. Fish and salamanders were double-pithed before removal of the eye. Eyes of an adult rhesus monkey were received already fixed in 10% formalin from the primate center at the University of California, Davis. For eyes from all species, anterior eyepoles and vitreous were cut away. The eyecups of all species except monkey were bathed in either 2% or 4% paraformaldehyde made in 0.1 M sodium phosphate buffer at pH 7.4 overnight. After fixation, the eyecups were kept in a 30% sucrose solution in phosphate buffer for at least 48 hr before being frozen in embedding medium. Sections 10 μm thick were cut on a cryostat and thaw-mounted onto glass slides (Fisherbrand Superfrost/Plus, Fisher). All procedures used in this study were approved by the Animal Care Committee of the University of California, San Diego and conform to the guidelines of the National Institutes of Health on the Care and Use of Laboratory Animals.

Slide-mounted sliced retinas were washed in PBS and incu-

NEUROBIOLOGY

bated overnight at 4°C with the affinity-purified rabbit polyclonal CB1 receptor antibodies (20) (1:200 dilution for monkey and mouse tissue, 1:500 in chick, fish, and salamander tissue, made in PBS, with 0.3% Triton, 10% nonfat milk). After the overnight incubation, the sections were washed with PBS, and then incubated with lissamine rhodamine goat anti-rabbit antibodies (1:100, Jackson ImmunoResearch) for 90 min at room temperature. Finally, the tissues were washed with PBS and coverslipped with glycerine carbonate. Tissues prepared with 2% vs. 4% paraformaldehyde and tissues fixed for 6 hr (rather than overnight) yielded similar labeling.

For the calbindin/CB1 double-label studies, a 1:4,000 dilution of calbindin (Sigma) and CB1 (concentrations as above) antibodies were simultaneously applied to slide-mounted tissue. The calbindin antibody, made in mouse, then was detected with FITC (1:100) goat anti-mouse antibody (Jackson Laboratories) whereas the CB1 was detected as before by a lissamine rhodamine anti-rabbit antibody. In control experiments, CB1 and calbindin antibodies were omitted to determine the level of background labeling, which was typically low. As a further control, the immunizing protein (1–2 μg/ml) was preincubated and coincubated with the CB1 antibodies. In all cases, CB1 labeling was successfully blocked by inclusion of the immunizing protein. Preincubation and coincubation of CB1 antibody with the NH$_2$ terminus of CB2 (1–2 μg/ml) did not diminish labeling.

GC/MS. GC/MS analysis of endogenous cannabinoids was carried out as described (21), with minor modifications. Briefly, rapidly dissected rat retinas (average weight of ≈ 20 mg) were immersed in 3 ml of ice-cold methanol containing deuterium-labeled standards (i.e., [^{2}H$_4$]anandamide, [^{2}H$_4$]oleylethanolamide, [^{2}H$_4$]palmitylethanolamide, [^{2}H$_8$]-2-arachidonylglycerol), and homogenized. After acetone (6 ml) precipitation of proteins (30 min on ice), the supernatants were collected and reduced to approximately 3 ml under a stream of N$_2$. Lipids were extracted for 30 min with ice-cold chloroform (6 ml). Chloroform phases were separated by adding H$_2$O (1.5 ml), and fractionated by open-bed chromatography followed by normal-phase HPLC. Fractions containing endogenous cannabinoid lipids were treated with bis(trimethylsilyl)trifluoroacetamide for 30 min at room temperature and analyzed by electron-impact GC/MS in the selected-ion monitoring mode. Deuterated standards were prepared as described (21) or purchased from Deva Biotechnology (Hartboro, PA).

Retinal Slices and Whole-Cell Patch Clamp Recording. Retinal slices in larval tiger salamanders (*Ambystoma tigrinum*) were made in a manner similar to that reported by Werblin (22). The slices were viewed with differential interference contrast optics with a 40× water immersion objective. Patch recordings of identified retinal bipolar cells (the recorded cell was stained with a fluorescent dye, Calcein) were made by using an EPC-9 amplifier and HEKA software (HEKA Electronics, Lambrecht/Pfalz, Germany) with methods similar to those reported by Maguire *et al.* (23). After recording, the fluorescent cell was viewed with an Olympus confocal laser scanning microscope for morphological identification. Patch pipettes for whole-cell recording contained 104 mM K-gluconate, 12 mM KCl, 0.1 mM CaCl$_2$, 4 mM Hepes, 1 mM EGTA, 200 μg/ml amphotericin B, and calcein (0.5% solution). Standard Ringer's contained 120 mM NaCl, 2 mM KCl, 3 mM CaCl$_2$, 1 mM MgCl$_2$, 4 mM Hepes, 3 mM D-glucose. Ringer's to isolate calcium currents included 50 mM NaCl, 1 mM MgCl$_2$, 4 mM Hepes, 3 mM D-glucose, 40 mM tetraethylammonium, 10 mM BaCl$_2$.

Results

Though this antibody was made against rat CB1, it also delivered robust and extensive labeling in the retinas of the monkey,

mouse, chick, tiger salamander, and goldfish. The pattern of staining was similar in all species. Labeling was found in most layers of the retina and will be presented in order of prominence.

OPL. In the retina of the monkey, antibodies to CB1 intensely labeled the OPL with many roughly spherical- and pyramidal-shaped structures that resemble the synaptic terminals of photoreceptors: rod spherules and cone pedicles, respectively (Fig. 1 *c* and *d*). To determine whether CB1 was specifically located in cone pedicles, CB1 antibodies were coapplied with those against calbindin, a known marker for cone photoreceptors (24). These results are presented in Fig. 1 *c* and *d* for monkey. Calbindin, shown in green, stains the full extent of cones, from the outer segments to their terminals in the OPL. CB1 staining, shown in red, was almost exclusively confined to the pedicle of the cone where there was intense yellow double staining for both substances. This finding confirmed the presence of CB1 in the cone pedicles. The CB1 staining in monkey continued into the thinner pedicle stalk in monkey (Fig. 1*d*, arrowhead). We did not perform double-labeling studies in the mouse or rat to determine the presence of CB1 labeling in cones; however, in both species (Figs. 1*a* and 2*a*) we detected intense CB1 labeling in the distal OPL, suggesting the presence of CB1 in the synaptic terminals of rod and/or cone photoreceptors. In chick retina, where a double cone pedicle arises from a thick extension of the double cones, CB1 staining showed an abrupt boundary (Fig. 1*b*), suggesting that the receptor is structurally constrained in its cellular distribution. The pattern of labeling corresponded very closely to the three layers of cone photoreceptor pedicles (Fig. 1*b*). Labeling was most intense in the OPL layer most proximal to the photoreceptors, a layer devoted to the terminals of double cones (25) and rods, but also could be detected in smaller numbers in layers two and three of the OPL (Fig. 1*b*, small arrowheads). The spherules and pedicles were the most intensely labeled objects in most of the retinas we examined.

In the goldfish, CB1 labeling was detected in a pattern that appeared to correspond closely to the photoreceptor cone pedicles and rod spherules (Fig. 3*e*). CB1 labeling also was noted in the OPL of the salamander.

IPL. In most species CB1 labeling in the IPL was generally robust but diffuse with only slight apparent stratification. The IPL of the primate was labeled in a sparse pattern (Fig. 3*a*). CB1 labeling in the mouse and rat (not shown) had little indication of stratification but in the mouse appeared to be more intense close to the inner nuclear layer (INL) and ganglion cell layer (GCL, not shown). The IPL of the chick was faintly but distinctly stratified with more intense labeling close to the INL (Fig. 3*c*). In the goldfish and the salamander, the IPL was labeled without any obvious stratification. We did not see labeling of individual processes and as such were unable to assign the labeling to a particular cell type.

Photoreceptor Inner and Outer Segments and Outer Nuclear Layer. In the primate, only photoreceptor inner segments were labeled (Fig. 3 *a* and *b*). In the mouse retina, the photoreceptor layer is composed almost exclusively of rods. Mouse photoreceptor outer segments displayed an endogenous fluorescence; however, immunolabeling above the level of autofluorescence was apparent (not shown). The same was found to be true in the rat except that the labeling appeared in the inner rather than outer segments. Low levels of CB1 labeling also were detected in the outer segments of chick photoreceptors. Circular labeling near the tips of chick photoreceptors is caused by the presence of oil droplets but is not related to the presence of CB1. In the remaining species we did not detect labeling in the inner or outer segments above the level of autofluorescence. In every species
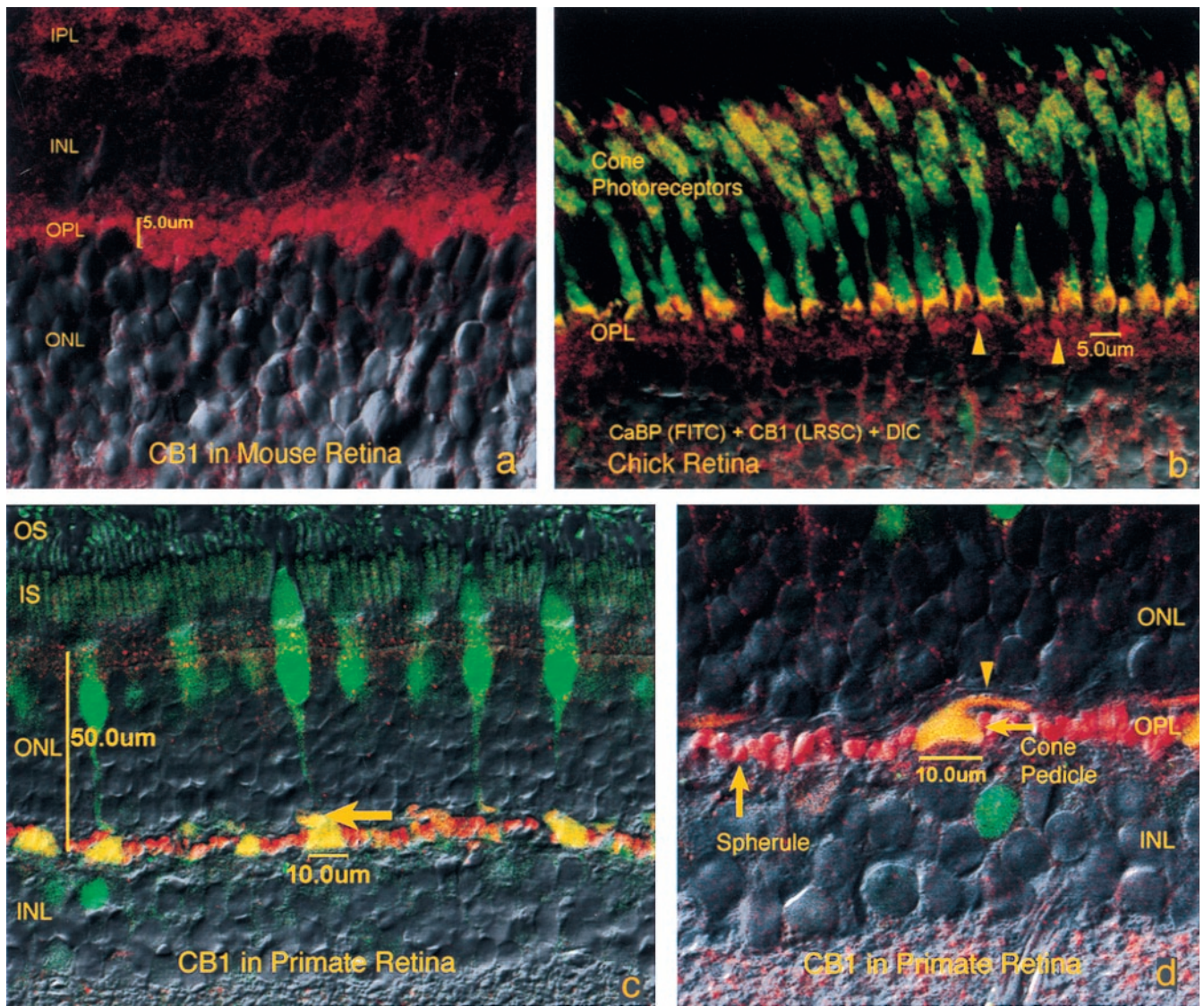
Fig. 1. CB1 is present in cone pedicles and rod spherules. Combined fluorescence and Nomarski micrograph. Photoreceptor inner segments (IS), outer nuclear layer (ONL), OPL, INL, IPL, and GCL. (*a*) CB1 labeling is found in the OPL of mouse retina in what probably correspond to spherules in the rod-dominated retina of the mouse. (*b*) Image of calbindin double-labeled with CB1 in chick retina. Cone photoreceptors are labeled in green (calbindin, CaBP). CB1 labeling is shown in red. Yellow double-labeling occurs within the pedicles of cone photoreceptors. Arrowheads indicate pedicle labeling in layers two and three of the chick OPL. (*c*) Labeling of the primate OPL shows very distinctly labeled pedicles (yellow, arrow) and spherules. (*d*) Higher magnification view of monkey OPL shows a calbindin/CB1 double-labeled cone pedicle as well as CB1 labeled rod spherules. Pedicle stalk is indicated by arrowhead. Magnifications: (*a* and *b*) ×900; (*c*) ×600; (*d*) ×950.

examined, the inner/outer segment labeling was much less pronounced than in the pedicles and spherules.
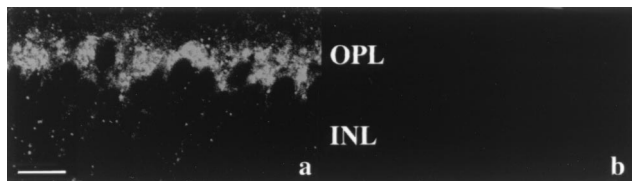

Fig. 2. Immunohistochemical localization of CB1 receptor in rat retina with preabsorption controls. Fluorescent images of rat retina (*a*) with control section showing CB1 labeling in the OPL. In the rat, as in all species examined, omission of CB1 antibody, or preabsorption with immunizing protein (*b*) blocked labeling. Both images were recorded at the same settings with a confocal microscope. (Scale bar = 10 microns.)

INL. Labeling in the INL was difficult to interpret in most of the species we examined. However, we saw what may have been CB1-positive amacrine cells in all species examined (Fig. 3 *a* and *c–e*). In the salamander, we saw faint INL somatic labeling that may correspond to Müller cells or amacrine cells (Fig. 3*d*).

GCL and the Retinal Axon Layer. Labeling of the CB1 receptor was found in the GCL and retinal axon layers of all species examined except fish. However, the most striking results were found in the salamander and chick (Fig. 3 *c* and *d*), where labeling was present both in ganglion cells and in the retinal axon layer and was particularly prominent in the chick where somatic labeling of ganglion cells was apparent.

Endogenous Cannabinoid Receptor Ligands. To determine whether endogenous cannabinoid lipids are present in retina, using GC/MS we analyzed lipid extracts of rapidly dissected rat
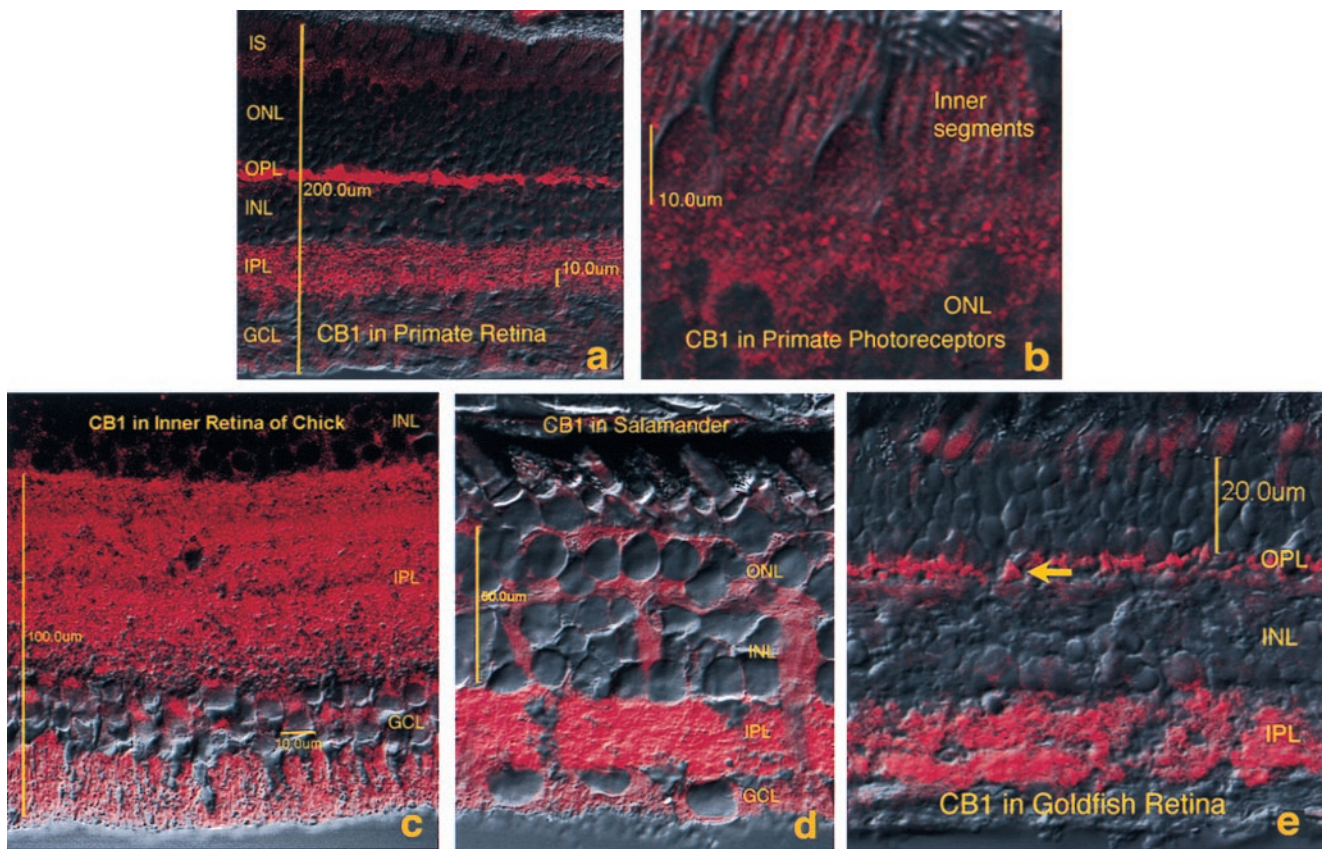
Fig. 3. CB1 labeling is found in a similar pattern in a wide range of vertebrate retinas. Combined fluorescence and Nomarski micrographs of transverse cross-sections of the retina. Photoreceptor inner segments (IS), outer nuclear layer (ONL), OPL, INL, IPL, GCL. (*a*) Overview of monkey retina, with pronounced labeling in OPL and IPL. (*b*) Higher magnification view of the photoreceptor layer of the primate retina, with CB1 labeling in the inner segments. (*c*) IPL of chick, showing robust labeling with some stratification. Somatic labeling in some ganglion and amacrine cells is also visible, as is labeling in ganglion cell axons. (*d*) Overview of retina of the tiger salamander. Labeling is present in OPL, INL, IPL, and GCL as well as ganglion cell axons. (*e*) Overall view of goldfish retina showing all layers. Labeling corresponds to rod spherules and cone pedicles (arrow) in the OPL. Labeling in the IPL is patchy because of tissue folding. Labeling in the photoreceptors is caused by autofluorescence. Magnifications: (*a*) ×230; (*b*) ×1,100; (*c*) ×450; (*d*) ×410; (*e*) ×625.

retinas. We observed components that were eluted from the GC at the retention time expected for 2-AG, PEA, and oleylethanolamide (OEA) (analyzed as trimethylsilylether derivatives, Fig. 4). These components coeluted with the corresponding deuterium-labeled standards. No detectable component was observed, however, at the retention time of anandamide (not shown). By comparison with the standard, we estimate that 2.97 ± 0.066 nmol of 2-AG, 130 ± 35 pmol of PEA, and 55 ± 5 pmol of OEA were recovered from 1 g of retinal tissue (mean + SEM; $n = 3$). These results indicate that rat retina contains detectable levels of 2-AG and PEA, two endogenous cannabinoid lipids, as well as of OEA, an acylethanolamide of as-yet-unknown function.

Cannabinoid CB1 Receptor Activation Inhibits Voltage-Gated Calcium Channel Current in Retinal Bipolar Cells of the Tiger Salamander. Voltage-gated calcium channel currents were elicited by depolarizing voltage steps from -70 mV to $+20$ mV in 10-mV increments (Fig. 5). Potassium currents were blocked by external tetraethylammonium (40 mM). Barium (10 mM) served as the charge carrier (replacing calcium) for the calcium channels. In all seven bipolar cells tested, the addition of 600 nM (four cells) or 1.5 μM (three cells) WIN 55212–2, a CB1 receptor agonist, blocked the sustained calcium-channel current (Fig. 5a). This calcium-channel current in bipolar cells of the tiger salamander has been shown to be carried by dihydropyridine-sensitive L-type calcium channels (23). The L-type current was restored by the addition of a synthetic CB1 receptor antagonist, SR141716A

(450 nM-1 μM). Subsequent wash of the agonist produced a substantial recovery of the calcium current. Mean peak amplitude of the control calcium current (0 mV) was -92 pA (SEM: 14pA, $n = 7$). Mean peak amplitude of the calcium current with WIN 55212–2 was -28pA (SEM: 18pA) corresponding to a 70% inhibition of peak current (significant by paired t test, $P < 0.05$). A photomicrograph of a representative calcein-filled bipolar cell, in which L-channel current was inhibited by WIN 55212–2 is shown in Fig. 5c.

Discussion

Immunolabeling for the CB1 receptor was found in the OPL and IPL of all species examined. Notably, prominent CB1 staining was found in the synaptic terminals of the photoreceptors of monkey, mouse, rat, chick, fish, and salamander, and the inner and/or outer segments of the photoreceptors of most species examined, strongly suggesting that cannabinoids act directly on the photoreceptors. All species appeared to possess CB1-positive amacrine cells. In the retinas of monkey, mouse, rat, chick, and salamander we also found labeling in ganglion cells and in the retinal axonal layer.

The presence of cannabinoid receptors in the retina raises a number of interesting questions about the possible role of this receptor in vision and the potential effects of cannabinoid receptor activation on retinal function. CB1 labeling in the cone pedicles of monkey, chick, fish, and salamander (and probably in the rod spherules of all species) constitutes the most prominent
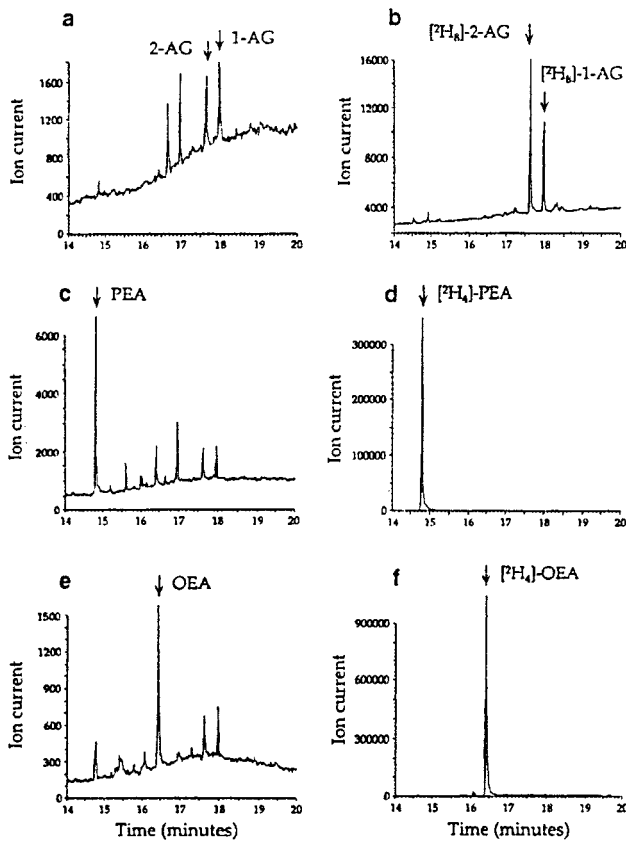
Fig. 4. Identification of 2-AG, PEA, and OEA in rat retina by GC/MS. Endogenous cannabinoid lipids 2-AG, PEA, and OEA were purified chromatographically from rat retina and analyzed by selected-ion monitoring GC/MS as bis trimethylsilylethers. For quantification, deuterium-labeled standards were added to all samples. Representative tracings for selected fragments characteristic of endogenous 2-AG (a, mass-to-charge ratio, $m/z = 432$), synthetic $[^2H_8]$-2-AG (b, $m/z = 440$), endogenous PEA (c, $m/z = 356$), synthetic $[^2H_4]$PEA (d, $m/z = 360$), endogenous OEA (e, $m/z = 382$), and synthetic $[^2H_4]$OEA (f, $m/z = 360$). Results are from one experiment and are typical of three independent experiments.

Fig. 5. Activation of CB1 receptors by WIN 55212–2 inhibits the voltage-gated calcium channel currents in retinal bipolar cell axon terminals. Recordings were made in the presence of tetraethylammonium (40 mM) and $BaCl_2$ (10 mM). (a) Traces represent L-type Ca^{2+} current in response to a depolarizing voltage step from −70 mV to +10 mV under control conditions, in the presence of CB1 agonist WIN 55212–2 [600 nM ($n = 4$) or 1.5 μM ($n = 3$)], with WIN 55212–2 and the selective CB1 antagonist SR141716A (450 nM-1 μM), and after wash. Shown is a hypothetical model cannabinoid receptor effect on glutamate release from bipolar cells via inhibition of L-type calcium currents. (b) Current-voltage relation shows a 70% inhibition of peak current by cannabinoids. Mean peak amplitude (at 0 mV, $n = 7$) is −92pA. Mean peak amplitude with WIN is −28pA. Treatment with CB1 antagonist or washing both restored currents. (c) Example of bipolar cell filled with fluorescent calcein dye during recording. Boundaries of the synaptic layers were determined by concurrent imaging with differential interference contrast optics.

pattern we have found. The roughly pyramid-shaped cone pedicles form the synaptic bouton of the photoreceptor, providing input to bipolar cells and horizontal cells. Spherules are the rod counterpart to pedicles. Pedicle labeling may represent a site of feedback modulation by other cells of the INL at the first layer of visual processing. The restricted labeling in cone pedicles was particularly evident in chick but also in the other species examined.

The electrophysiological data from the present study indicate that activation of CB1 receptors modulates voltage-gated L-type calcium channels in retinal bipolar cell axon terminals. Although the immunohistochemical data did not conclusively identify CB1 in bipolar cells, the staining pattern in the IPL is consistent with the electrophysiological data, suggesting that CB1 is present in the bipolar cell axon terminals. Because L-type channels control glutamate release at these synapses (23) this finding suggests that cannabinoids modulate glutamatergic synaptic transmission between the second-order bipolar and amacrine cells and the downstream ganglion cells. Further, given the presence of CB1 receptors on photoreceptor synaptic terminals, glutamatergic synaptic transmission between photoreceptors and second-order cells also may be modulated by cannabinoids. If so, then given that photoreceptors respond to light signals by reducing gluta-
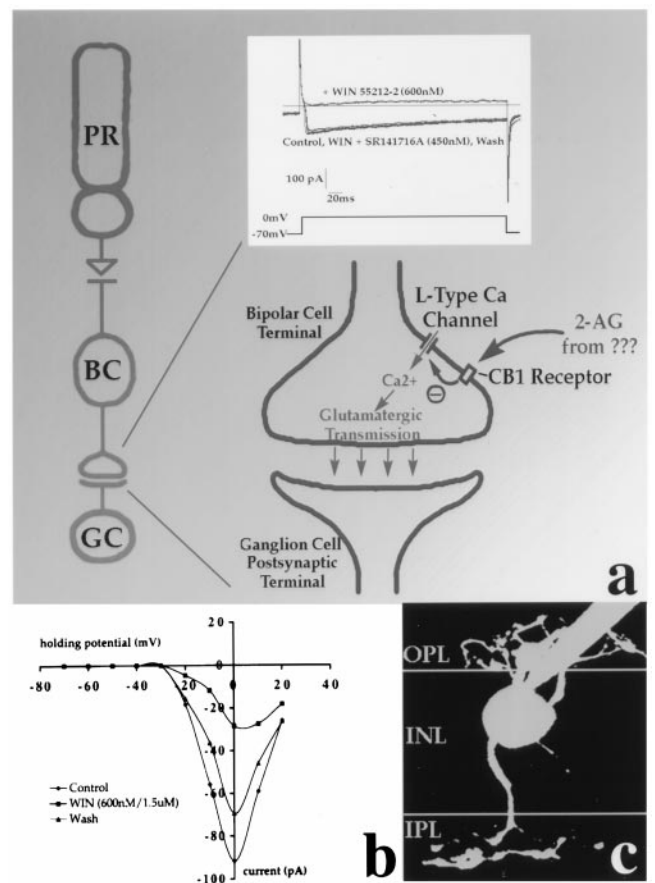
mate release a predicted effect of cannabinoids might be to mimic the light activation of photoreceptors.

The presence of 2-AG, an endogenous ligand for CB1 receptors, clearly reinforces the notion of a cannabinoid receptor-based neuromodulatory system in retina. The fact that anandamide levels were not detectable by our method, which reliably measures quantities of anandamide as low as 0.4 pmol/sample, is surprising. Because anandamide is likely produced "on demand" (26, 27), it is possible that static levels such as those determined in the present experiments may only partially reflect the biosynthetic capacity of retinal tissue. Less likely, hydrolysis by anandamide amidohydrolase, which is present in the retina (28), could account for our negative result. It should be noted, however, that anandamide has been detected in other areas of the brain with high levels of the amidohydrolase. Whether the cannabinoid signaling system of the retina differs from the rest of the brain (i.e., whether retina makes use only of 2-AG as an endogenous ligand) is an interesting issue that remains to be

addressed in greater detail. We were unable to determine which cell types are responsible for PEA and 2-AG release. Localization of PEA and 2-AG will be fundamental to an understanding of their roles in any retinal cannabinoid neuromodulatory system and should be a focus of future investigations. The presence of PEA, a CB2-like receptor agonist (19, 29), is interesting in view of the recent localization of CB2 receptor mRNA in retina (30).

These immunohistochemical, biochemical, and electrophysiological observations, combined with those of other investigators (16–18), give us reason to believe that CB1 receptors and possibly CB2 receptors, acting as part of a novel signaling system in the retina, play a substantive role in retinal function by inhibiting the calcium currents in bipolar cells that are responsible for calcium-dependent glutamatergic synaptic transmission (22). Most of our results appear to be consistent across a wide range of vertebrate species, a conservation of form that may reflect a conservation of function. Most users of marijuana and hashish will readily describe perceived visual effects. Although our results open the possibility of a retinal cannabinoid role in vision, any of the diverse reported visual effects may be the result of action on CB1 receptors present in higher brain regions dedicated to vision (20). As such, any hypothesized retinal cannabinoid effects on vision must await further study. We suggest that studying the role of cannabinoid receptors in the retina will yield a greater understanding of what promises to be a novel retinal signaling system and possibly shed light on visual effects of marijuana use. We further hope that this work will offer opportunities to relate endocannabinoid action with a specific function in the body.

1. Devane, W. A., Hanus, L., Breuer, A., Pertwee, R. G., Stevenson, L. S., Griffin, G., Gibson, D., Mandelbaum, A., Etinger, A. & Mechoulam, R. (1992) *Science* **258,** 1946–1949.
2. Kiplinger, G. F., Manno, J. E., Rodda, B. E. & Forney, R. B. (1971) *Clin. Pharmacol. Ther.* **12,** 650–657.
3. Rose, S., Dwyer, W. & Yehle, A. (1979) *Pharmacol. Biochem. Behav.* **10,** 851–853.
4. Moskowitz, H., Sharma, S. & McGlothlin, W. (1972) *Percept. Motor Skills* **35,** 875–882.
5. Matsuda, L. A., Lolait, S. J., Brownstein, M. J., Young, A. C. & Bonner, T. I. (1990) *Nature (London)* **346,** 561–564.
6. Herkenham, M., Lynn, A. B., Johnson, M. R., Melvin, L. S., de Costa, B. R. & Rice, K. C. (1991) *J. Neurosci.* **11,** 563–583.
7. Stella, N., Schweitzer, P. & Piomelli, D. (1997) *Nature (London)* **388,** 773–778.
8. Poling, J. S., Rogawski, M. A., Salem, N., Jr. & Vicini, S. (1996) *Neuropharmacology* **35,** 983–991.
9. Mackie, K., Lai, Y., Westenbroek, R. & Mitchell, R. (1995) *J. Neurosci.* **15,** 6552–6561.
10. Deadwyler, S. A., Hampson, R. E., Mu, J., Whyte, A. & Childers, S. (1995) *J. Pharmacol. Exp. Ther.* **273,** 734–743.
11. Zeltser, R., Seltzer, Z., Eisen, A., Feigenbaum, J. J. & Mechoulam, R. (1991) *Pain* **47,** 95–103.
12. Derkinderen, P., Toutant, M., Burgaya, F., Le Bert, M., Siciliano, J. C., de Franciscis, V., Gelman, M. & Girault, J.-A. (1996) *Science* **273,** 1919–1922.
13. Martin, W. J., Hohmann, A. G. & Walker, J. M. (1996) *J. Neurosci.* **16,** 6601–6611.
14. Terranova, J. P., Michaud, J. C., Le Fur, G. & Soubrié, P. (1995) *Naunyn Schmiedebergs Arch. Pharmacol.* **352,** 576–579.
15. Stefano, G. B., Salzet, B., Rialas, C. M., Pope, M., Kustka, A., Neenan, K., Pryor, S. & Salzet, M. (1997) *Brain Res.* **763,** 63–68.
16. Schlicker, E., Timm, J. & Göthert, M. (1996) *Naunyn Schmiedebergs Arch. Pharmacol.* **354,** 791–795.
17. Buckley, N. E., Hanson, S., Harta, G. & Mezey, E. (1998) *Neuroscience* **82,** 1131–1149.
18. Porcella, A., Casellas, P., Gessa, G. L. & Pani, L. (1998) *Brain Res. Mol. Brain. Res.* **58,** 240–245.
19. Facci, L., Dal Toso, R., Romanello, S., Buriani, A., Skaper, S. D. & Leon, A. (1995) *Proc. Natl. Acad. Sci. USA* **92,** 3376–3380.
20. Tsou, K., Brown, S., Sañudo-Peña, M. C., Mackie, K. & Walker, J. M. (1998) *Neuroscience* **83,** 393–411.
21. Giuffrida, A. & Piomelli, D. (1998) *FEBS Lett.* **422,** 373–376.
22. Werblin, F. (1978) *J. Physiol. (London)* **294,** 613–626.
23. Maguire, G., Maple, B., Lukasiewicz, P. & Werblin, F. (1989) *Proc. Natl. Acad. Sci. USA* **86,** 10144–10147.
24. Hamano, K., Kiyama, H., Emson, P. C., Manabe, R., Nakauchi, M. & Tohyama, M. (1990) *J. Comp. Neurol.* **302,** 417–424.
25. Mariani, A. P. & Leure-duPree, A. E. (1978) *J. Comp. Neurol.* **182,** 821–837.
26. Di Marzo, V., Fontana, A., Cadas, H., Schinelli, S., Cimino, G., Schwartz, J. C. & Piomelli, D. (1994) *Nature (London)* **372,** 686–691.
27. Cadas, H., di Tomaso, E. & Piomelli, D. (1997) *J. Neurosci.* **17,** 1226–1242.
28. Matsuda, S., Kanemitsu, N., Nakamura, A., Mimura, Y., Ueda, N., Kurahashi, Y. & Yamamoto, S. (1997) *Exp. Eye. Res.* **64,** 707–711.
29. Calignano, A., La Rana, G., Giuffrida, A. & Piomelli, D. (1998) *Nature (London)* **394,** 277–281.
30. Lu, Q. J., Straiker, A. S., Lu, Q. X. & Maguire, G. M. (2000) *Visual Neurosci.*, in press.